ELSEVIER

Journal of Power Sources 102 (2001) 172–177

JOURNAL OF POWER SOURCES

www.elsevier.com/locate/jpowsour

Electrochemical characteristics of Pt–WO_3/C and Pt–TiO_2/C electrocatalysts in a polymer electrolyte fuel cell

Joongpyo Shim[a,*], Chang-Rae Lee[a], Hong-Ki Lee[b], Ju-Seong Lee[c], Elton J. Cairns[a]

[a]*Environmental Energy Technologies Divison, Lawrence Berkeley National Laboratory, Berkeley, CA 94720, USA*
[b]*Department of Chemical Engineering, Woosuk University, Chunbook, South Korea*
[c]*Department of Industrial Chemistry, Hanyang University, Seoul 133-791, South Korea*

Received 12 March 2001; accepted 6 April 2001

Abstract

The electrochemical characteristics and the catalytic activity of Pt–tungsten oxide and Pt–titanium oxide catalysts in polymer electrolyte fuel cell were investigated by cyclic voltammetry and in fuel cells. Fuel cell performances for those catalysts at 80°C with humidified hydrogen and oxygen increased with increasing added oxide content in the catalysts up to a certain content. Adsorption characteristics for hydrogen and oxygen on the surface of platinum were greatly influenced by added oxide content in the catalysts. It was also obtained that the electrochemically active surface area of these catalysts was influenced by their oxide content. © 2001 Elsevier Science B.V. All rights reserved.

Keywords: Polymer electrolyte fuel cell; Tungsten oxide; Titanium oxide; Electrocatalyst

1. Introduction

Many researchers have investigated the alloying of platinum with transition metals to improve the catalytic activity and increase the tolerance for carbon monoxide in polymer electrolyte fuel cells (PEFCs). Pt–Co, Pt–Ni, Pt–Fe and Pt–Ru catalysts supported on conductive materials such as carbon black showed high activity for the oxygen reduction reaction and high CO-tolerance in PEFCs [1–3]. However, these Pt alloy materials have to be sintered above 700°C to prepare homogeneous alloy that are stable in acidic or alkaline media.

Tungsten oxides are stable in acidic solution and are prepared easily from ammonium or sodium tungstate and tungsten metal. Hobbs and Tseung observed that the rate for hydrogen oxidation in acidic solution increased by the use of Teflon-bonded Pt supported on WO_3, since hydrogen spilled over onto the surface of the hydrogen tungsten bronze, freeing these Pt sites for further chemisorption of hydrogen [4]. Savadogo and Beck reported that the electrocatalytic properties of the oxygen reduction reaction, exchange current density and mass activity of 5%Pt–40%WO_3 based electrode in phosphoric acid at 180°C were twice as high as those of 10%Pt on carbon [5].

In this paper, the catalytic activity of Pt–WO_3 and Pt–TiO_2 supported on carbon black in a polymer electrolyte fuel cell was investigated. Tungsten oxide and titanium oxide were easily impregnated on carbon black by chemical reaction from sodium tungstate and titanium isopropoxide, respectively. The electrochemical characteristics of both catalysts were investigated in acidic polymer electrolyte by cyclic voltammetry.

2. Experimental

Pt–WO_3/C catalysts were prepared from 10% platinum on carbon (E-TEK Co.) and sodium tungstate (Na_2WO_4) as the precursor of WO_3. First, sodium tungstate was dissolved in an aqueous Pt/C dispersion, and then excess conc. hydrochloric acid was added to this solution. Nanoscale tungsten oxide particles were produced by the reaction of sodium tungstate with hydrochloric acid [6]. The solution was stirred for 24 h at ambient temperature to adsorb tungsten oxide on the carbon black. The suspension was washed, and then dried at 60°C for 6 h.

Pt–TiO_2/C catalysts were prepared from 10% platinum on carbon (E-TEK Co.) and titanium isopropoxide as the precursor of TiO_2. First, Pt/C and titanium isopropoxide were suspended in ethanol. Excess deionized water was added to this solution, causing the hydrolysis of titanium

* Corresponding author. Tel.: +1-510-486-7257; fax: +1-510-486-7303.
E-mail address: jpshim@lbl.gov (J. Shim).

PII: S0378-7753(01)00817-5

isopropoxide. The hydrolyzed TiO_2 particles were deposited on the Pt/C particles.

Nafion 115 membrane was used as the polymer electrolyte (Dupont, thickness 0.125 mm, equivalent weight 1100 g/mol). The Nafion membrane was pretreated in a 5% H_2O_2 solution and 0.5 M H_2SO_4 at 70–80°C for 1 h each.

The catalyst ink was prepared by mixing catalyst powder, Nafion solution (Dupont, 5% solution, equivalent weight 1100 g/mol) and solvent (mixture of water and isopropyl alcohol). The catalyst ink was painted onto wet-proofed carbon cloth, and dried at 60°C in air to remove solvent (alcohol and water) from the catalyst ink. The gas diffusion electrodes prepared as described above were hot-pressed onto the pretreated Nafion 115 at 100°C for 120 s to make membrane electrode assembly.

The performance measurements for the cell were carried out using on electronic load box (Dae Gil Elec. Co., EP-1200). For cyclic voltammetry, hydrogen was passed through the anode region and nitrogen through the cathode region for 30 min. Cyclic voltammetry measurements using a Potentiostat/Galvanostat (EG&G Parc., 273A) were recorded to determine the electrochemically active surface area. The potential range and the scan rate were 0.04–1.2 V (versus RHE) and 20 mV/s, respectively. The electrochemically active surface area of the electrode was obtained from the charge for hydrogen desorption from the Pt electrocatalyst.

XRD analysis of the Pt–WO_3/C and Pt–TiO_2/C catalysts was performed using a Rigaku diffractometer (RAD-C 4037A1) with a Cu Kα radiation source to characterize the structure of WO_3 and TiO_2 on carbon.

3. Results and discussion

The electrochemical characteristics of Pt–WO_{3-x}/C catalysts were investigated for the electrochemical oxidation of methanol by Shukla et al. [7]. They reported on WO_{3-x} powders prepared from the reduction of $(NH_4)_6H_2W_{12}O_{40}$ by sodium borohydride ($NaBH_4$). The reduced WO_{3-x} powders were adsorbed on Pt/C powder physically. In this study, tungsten oxide was deposited on carbon black by chemical reaction of sodium tungstate with hydrochloric acid. Fig. 1 shows the XRD patterns of Pt–WO_3/C powders prepared from sodium tungstate. As shown in Fig. 1, we observed that the tungsten oxides were crystalline WO_3 powder. As the content of tungsten oxide was increased, the peak intensity also increased. We could not detect any other tungsten compounds, such as H_xWO_3, H_2WO_4 or Na_xWO_{4-x}.

Fig. 2 shows XRD patterns of Pt–TiO_2/C catalysts prepared from titanium isopropoxide by hydrolysis. We could confirm the peak of titanium oxide for the Pt–20%TiO_2 catalyst, but the other catalysts did not show sharp peaks of titanium oxide in Fig. 2. We think the particles of titanium oxide are very fine nanocrystals or have an amorphous

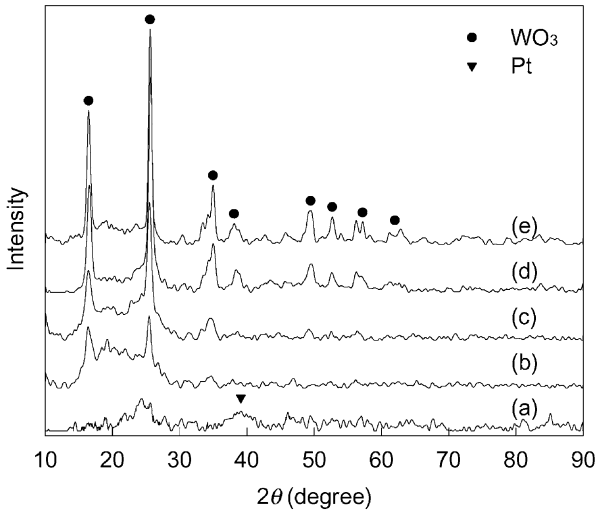

Fig. 1. XRD patterns of Pt–tungsten oxide catalysts on carbon black: (a) Pt/C; (b) Pt–3%WO_3/C; (c) Pt–5%WO_3/C; (d) Pt–10%WO_3/C; (e) Pt–20%WO_3/C.

structure. In Fig. 2, we could not detect any peaks that would indicate the alloying of platinum and titanium. The broad peak at ca. 25° is the reflection of carbon black. Beard and Ross reported that ordered Pt_3Ti alloy catalysts could be prepared by heat-treatment above 900°C. They found a titanium compound on carbon black was amorphous TiO_2 for a sample that received no heat-treatment sample [8].

Fig. 3 shows the performance of H_2/O_2 cells with Pt–WO_3/C catalysts as a function of tungsten oxide content. It is clear that the cell performance is influenced by the oxide content in the catalyst. Performance increased with increasing tungsten oxide content up to 5%, but then decreased. No mass transfer limitation was observed at cell potentials about 0.5 V. This means tungsten oxide particles did not affect mass transfer of the humidified reactant gases, hydrogen and

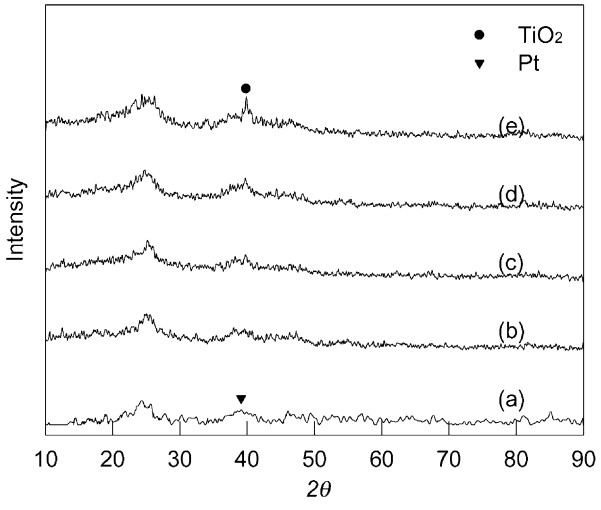

Fig. 2. XRD patterns of Pt–titanium oxide catalysts on carbon black: (a) Pt/C; (b) Pt–5%TiO_2/C; (c) Pt–10%TiO_2/C; (d) Pt–15%TiO_2/C; (e) Pt–20%TiO_2/C.

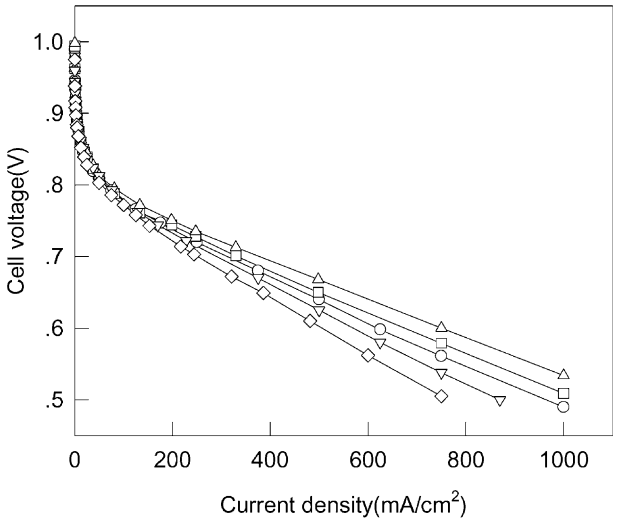

Fig. 3. Current–potential curves of Pt–WO_3/C catalysts; 0.3 mg Pt/cm^2, cell temperature 80°C, H_2/O_2 = 90/85°C, gas pressure H_2/O_2 = 1/1 atm: (○) Pt/C; (□) Pt–3%WO_3/C; (△) Pt–5%WO_3/C; (▽) Pt–10%WO_3/C; (◇) Pt–20%WO_3/C.

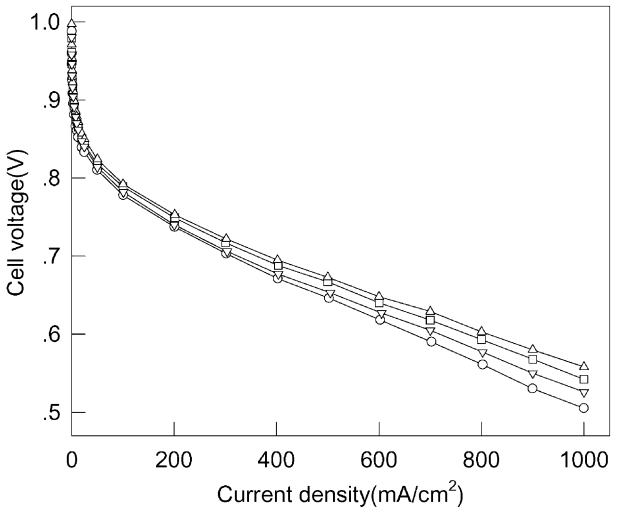

Fig. 4. Current–potential curves of Pt–TiO_2/C catalysts; 0.3 mg Pt/cm^2, cell temperature 80°C, H_2/O_2 = 90/85°C, gas pressure H_2/O_2 = 1/1 atm: (○) Pt/C; (□) Pt–10%TiO_2/C; (△) Pt–15%TiO_2/C; (▽) Pt–20%TiO_2/C.

oxygen, and that the electrode structures were not adversely changed by the addition of the oxide materials. The possible dissolution of tungsten oxide in the acidic electrolyte under various operating conditions and possible methods of reducing its dissolution was investigated by several researchers. Randin reported that tungsten oxide for electrochromic films is slightly soluble in sulfuric acid [9]. To improve the stability of tungsten oxide, Chen and Tseung investigated Nafion coated Pt/WO_3 electrodes. They reported that by coating Pt/WO_3 electrodes with a thin Nafion layer, the solubility of tungsten oxide is reduced significantly, electrode performance is stable, and electrode activity for the oxidation of methanol and formic acid is not observed [10]. We could not detect any decrease of cell performance during cell operation for more than 48 h or a decrease of peak intensity after more than 50 cycles in the cyclic voltammograms (CV).

Fig. 4 shows the curves for the cell performance of the Pt–TiO_2/C catalysts in the polymer electrolyte fuel cell. As the content of titanium oxide in the catalyst increases to 20%, the performance of all of the catalysts with titanium oxide was higher than that of the pure platinum catalyst unlike the case for Pt–WO_3/C catalysts. The cell performance improved with increasing titanium oxide content up to 15%, but decreased at 20%. It was observed that both tungsten oxide and titanium oxide can improve the cell performance.

Fig. 5 shows the CV of pure platinum, platinum–tungsten oxide and –titanium oxide catalysts. Between 0.04 and 0.4 V, hydrogen atoms are adsorbed on the cathodic sweep, and desorbed on the anodic sweep. Above 0.8 V on the anodic sweep, oxide film is formed on the surface of platinum catalysts. And then, on the cathodic sweep, oxide film is removed by reduction [11]. We can observe the phenomenon for the adsorption and desorption of hydrogen atoms and calculate the electrochemical surface area of platinum from the region of hydrogen desorption. Also we can obtain information on the formation of the oxide film on the surface of platinum from the region for the reduction of the oxide film [12,13]. Electrochemical characteristics for hydrogen adsorption/desorption in the CV profile depend on the particle size of platinum. As shown in Fig. 5, peaks that are corresponded to weakly- and strongly-bonded hydrogen are not observed clearly except for Pt–WO_3/C catalyst. Peaks for only weakly-bonded hydrogen are observed at about 0.15–0.20 V. That may be due to the fact that the platinum particles are small (2.5 nm) and have many corners and edges [14].

For the Pt–WO_3/C catalyst, peaks for hydrogen adsorption/desorption are observed at about 0.3 and 0.35 V in the

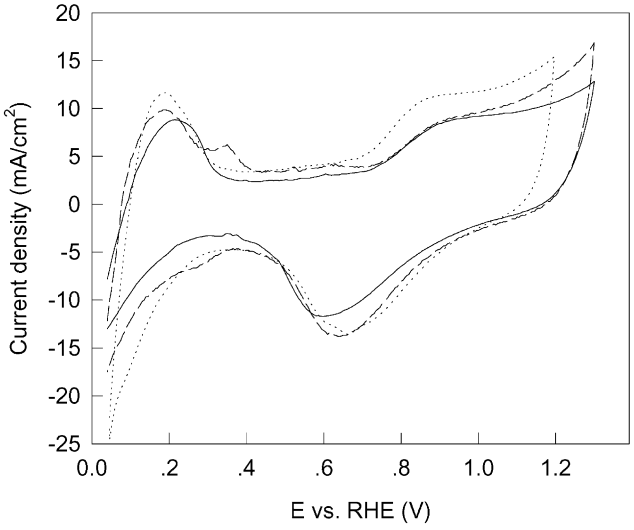

Fig. 5. Cyclic voltammograms of Pt–WO_3/C and Pt–TiO_2/C catalysts at 20 mV/s: (—) Pt/C; (- - -) Pt–5%WO_3/C; (· · ·) Pt–15%TiO_2/C.

cathodic and anodic sweeps, respectively. We think that those peaks are not for strongly-bonded hydrogen on platinum. That is the reason hydrogen atom is strongly bonded on platinum at 0.22–0.28 V [15] and there are not any peaks at that region in pure Pt and Pt–TiO_2/C. Many researchers have studied the electrocatalytic properties and electrochemical characteristics of Pt–tungsten oxide in acidic solution. It's reported tungsten oxide could form two stable hydrogen tungsten bronzes, $H_{0.18}WO_3$ and $H_{0.35}WO_3$, and substoichiometric oxides, WO_{3-y}, by reaction with hydrogen [16].

$$WO_3 + xH^+ + xe^- = H_xWO_3 \quad (0 < x < 1) \tag{1}$$

$$WO_3 + 2yH^+ + 2ye^- = WO_{3-y} + yH_2O \quad (0 < y < 1) \tag{2}$$

But, at Pt–tungsten oxide catalysts, the reaction mechanism for the adsorption of hydrogen can be postulated as the following chemical reaction [17–19].

Normal Pt mechanism

$$2Pt + H_2 = 2PtH_{ads} \tag{3}$$

$$PtH_{ads} = Pt + H^+ + e^- \tag{4}$$

Bronze route

$$xPtH_{ads} + WO_3 = Pt + H_xWO_3 \tag{5}$$

$$H_xWO_3 = xH^+ + WO_3 + xe^- \tag{6}$$

Kulesza and Faulkner reported there were well defined reduction peaks at −0.03 and −0.17 V (versus SCE) at Pt–W(VI, V) oxide on graphite in cyclic voltammetry [20]. They assigned those peaks to hydrogen tungsten bronze formation and also they reported those peaks coincided with two adsorption/desorption peaks for hydrogen on polycrystalline Pt. In this study, peaks at about 0.3 V (cathodic sweep) and 0.35 V (anodic sweep) for Pt–WO_3/C could be assigned to the formation of hydrogen tungsten bronze, but the peak potentials were shifted more positive than that in the results of Kulesza and Faulkner. We think further study is needed concerning the formation of hydrogen tungsten bronze on Pt–WO_3 supported carbon black.

The electrochemical surface areas for pure platinum, Pt–WO_3/C and Pt–TiO_2/C are shown in Tables 1 and 2. The electrochemical surface area of platinum catalyst was calculated from the coulombic charge for hydrogen desorption, assuming a value of 220 μC/cm^2 Pt for the oxidation of adsorbed atomic hydrogen on a smooth Pt surface [21]. In Tables 1 and 2, the electrochemically active surface area of Pt–oxide catalysts was higher than pure platinum catalysts.

Table 2
Electrode kinetic parameters of Pt–TiO_2/C at 80°C

	Tafel slope (mV/dec)	Surface area (cm^2 Pt/cm^2)[a]	Mass activity (mA/mg Pt)[b]
Pt/C	60	159	69
Pt–5%TiO_2/C	55	200	100
Pt–10%TiO_2/C	56	206	133
Pt–15%TiO_2/C	57	242	166
Pt–20%TiO_2/C	57	182	116

[a] Electrochemically active surface area.
[b] At 0.9 V of cell voltage.

In Pt–WO_3/C, the active surface area increased with increasing content of tungsten oxide. The total charge for hydrogen desorption includes the formation of hydrogen tungsten bronze. When the coulombic charge for formation of hydrogen tungsten bronze is removed from total charge, the electrochemically active surface area slightly decreases with increase of tungsten oxide amount over 10%, but is still higher than pure platinum. The Tafel slope for the oxygen reduction reaction decreased for tungsten oxide amount up to 5%, but increased at 10 and 20% tungsten oxide. The catalyst mass activity also showed an increase on the addition of tungsten oxide up to 5%, but a decrease above 10% of tungsten oxide.

We could not observe any peaks for the interaction of titanium with hydrogen or oxygen in the cyclic voltammogram of Pt–TiO_2/C. The electrochemically active surface areas of all Pt–TiO_2/C were higher than for pure platinum, as for Pt–WO_3/C in Table 1. The Tafel slope showed a lower value than pure platinum, up to 20% titanium oxide. The mass activity of all catalysts showed a higher value than pure platinum and its maximum value was at Pt–15%TiO_2/C catalyst.

Hydrogen desorption potentials for Pt–WO_3/C and Pt–TiO_2/C were generally lower than for pure platinum, as shown in Fig. 6. The hydrogen desorption potential of Pt–TiO_2/C decreased up to 20% of titanium oxide, but that of Pt–WO_3/C was decreased up to 10% of tungsten oxide and then increased at 20% again. That difference of the curve

Table 1
Electrode kinetic parameters of Pt–WO_3/C at 80°C

	Tafel slope (mV/dec)	Surface area (cm^2 Pt/cm^2)[a]	Surface area (cm^2 Pt/cm^2)[b]	Mass activity (mA/mg Pt)[c]
Pt/C	60	159		69
Pt–3%WO_3/C	58	216	176	135
Pt–5%WO_3/C	56	239	194	208
Pt–10%WO_3/C	67	247	190	59
Pt–20%WO_3/C	74	249	186	45

[a] Electrochemically active surface area.
[b] Surface area removed charge for hydrogen adsorbed on tungsten oxide.
[c] At 0.9 V of cell voltage.

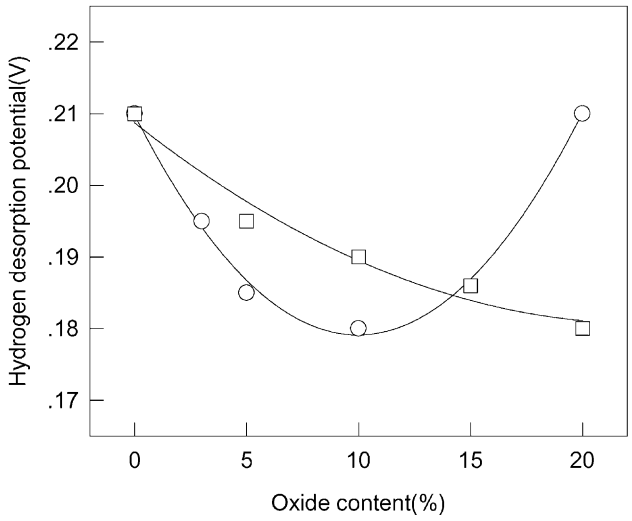

Fig. 6. Hydrogen desorption potential on oxide content in Pt–WO_3/C and Pt–TiO_2/C based on cyclic voltammograms: (○) Pt–WO_3/C; (□) Pt–TiO_2/C.

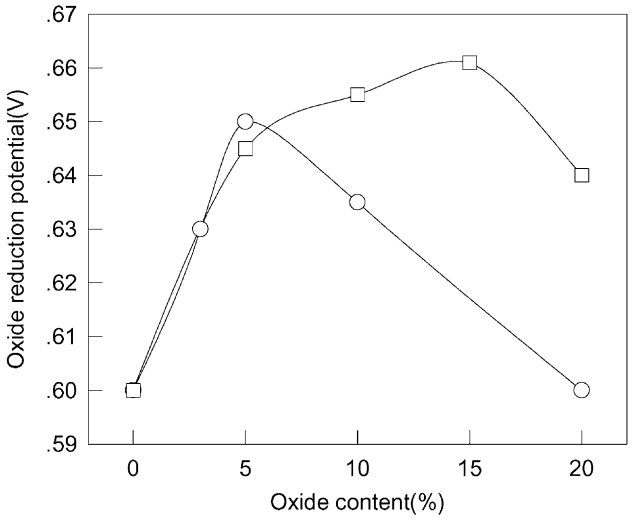

Fig. 8. Oxide reduction potential on oxide content in Pt–WO_3/C and Pt–TiO_2/C based on cyclic voltammograms: (○) Pt–WO_3/C; (□) Pt–TiO_2/C.

shapes may be due to the size and the crystal structure of the added oxide particles. We could observe that tungsten oxide was crystalline but the titanium oxide was amorphous (from XRD in Figs. 1 and 2). In platinum alloy catalysts, the hydrogen desorption potential was increased by alloying with transition metals because the crystal structure and lattice parameter of platinum were changed [13]. In this study, those of platinum are not changed after adding the oxide particles, but the hydrogen desorption potential of platinum–metal oxide catalysts is decreased. This means that the strength of hydrogen adsorption on the surface of platinum is reduced by interaction of the oxide with the hydrogen. Also, it means that platinum can release adsorbed hydrogen atom easily.

Figs. 7 and 8 show the variation of the Pt oxide reduction potential and charge, (based on the CV's) with the oxide content. The maximum values of both catalysts for the oxide reduction charge are the same, but the oxide content in the catalysts is different. The peak area of Pt–WO_3/C and Pt–TiO_2/C for oxide reduction were higher than for pure Pt/C. This means that the number of active sites, on which oxygen species or –OH species are adsorbed, is increased by the addition of metal oxide. That may be the reason that the cell performance of Pt–WO_3/C and Pt–TiO_2/C catalysts is higher than for pure platinum. Oxide reduction potentials for Pt–WO_3/C and Pt–TiO_2/C show volcano type behavior on the content of oxide. It is observed that the metal oxide in the catalyst increases the reduction potential of the oxide formed on the surface of platinum. This means that metal oxides can weaken the strength of adsorption of oxygen species on platinum. This is similar to the behavior for the adsorption of hydrogen on the surface of platinum. We can conclude that metal oxides near platinum can weaken the strength of the adsorption of hydrogen and oxygen on the surface of platinum.

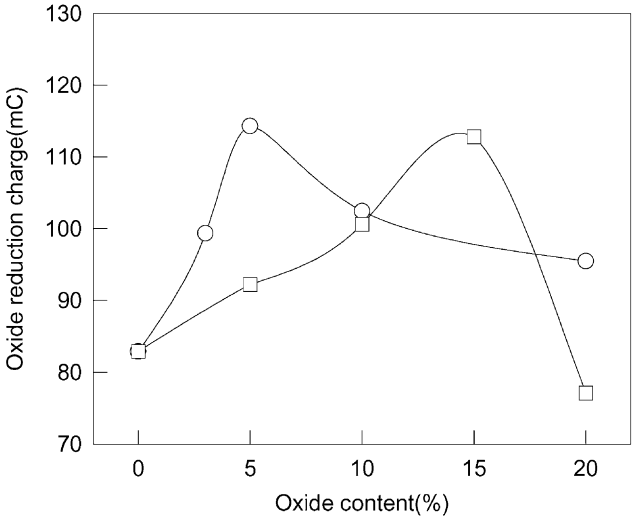

Fig. 7. Oxide reduction coulomb on oxide content in Pt–WO_3/C and Pt–TiO_2/C based on cyclic voltammograms: (○) Pt–WO_3/C; (□) Pt–TiO_2/C.

The improvement of cell performance and the weak adsorption of hydrogen and oxygen can be explained by the synergetic effect of the adlineation model and the spillover model, proposed by Fleischmann et al. [22] and Boudart et al. [23], respectively. Also, McHardy and Bockris explained the electrocatalysis of oxygen reduction using those models at sodium tungsten bronze with platinum [24]. The adlineation model is that the active sites in a two-phase catalyst are the linear boundaries between the phases. The spillover model is the surface diffusion of reaction intermediates from one catalyst to other catalyst. In Tables 1 and 2, we can see the increase of electrochemically active surface area for Pt–WO_3/C and Pt–TiO_2/C catalysts. The intrinsic catalytic activity of platinum wasn't changed after the addition of oxide materials because of no heat-treatment. Also, tungsten oxide and titanium oxide have no or very low activity compared to pure platinum. These oxide materials

have an effect on the variation of active surface area of the catalysts. We think that new active sites are formed at the interface between platinum and the added oxide materials according to the adlineation model.

In Fig. 6, the hydrogen desorption potential decreases with increasing oxide content. As mentioned above, this may mean that the adsorption strength of hydrogen on the surface of platinum is weakened by the added oxide materials. It was observed that the peak, which is assumed to be produced by the spillover model for the reaction of hydrogen with tungsten oxide in cyclic voltammogram of Fig. 5. The coulombic charge and potential for oxide reduction on the surface of platinum increases with increasing oxide content as shown in Figs. 7 and 8. This means that the oxide materials have an effect on the increase of active surface area and the weakening of the adsorption strength of oxygen species by a synergistic effect according to both adlineation and spillover models. But, we could not find any additional peaks for reaction of oxygen species with the added oxide materials.

The cell performance of the polymer electrolyte fuel cell is more influenced by the oxygen reduction reaction than hydrogen oxidation because the polarization for the former is bigger than for the latter. The results of coulombic charge and potential for oxide reduction in Figs. 7 and 8 are very similar to the cell performance curves of Pt–WO_3/C and Pt–TiO_2/C in Figs. 3 and 4. Cell performances at Pt–10%WO_3/C and Pt–20%WO_3/C showed lower performance than the pure platinum catalysts. We could not explain the reason for the decreased performance of those catalysts by the behavior of the oxide reduction charge and potential in Figs. 7 and 8, in spite of the higher active surface area than pure platinum. The decrease of cell performance for those catalysts might be influenced by complex factors for the increase of hydrogen desorption potential and both the decrease of oxide reduction charge and potential.

4. Conclusion

Pt–WO_3/C and Pt–TiO_2/C catalysts were prepared easily by chemical reaction at room temperature from sodium tungstate and titanium isopropoxide, respectively. Some of those catalysts showed higher fuel cell performance than pure platinum catalyst. By cyclic voltammetry, it was observed that the electrochemically active surface areas of Pt–WO_3/C and Pt–TiO_2/C catalysts were increased significantly. The adsorption strength of hydrogen and oxygen on the surface of platinum were weakened by the presence of these oxide materials in the catalysts. The improvement of fuel cell performance, the increase of electrochemically active surface area and variation of adsorption of hydrogen and oxygen were caused by synergistic effects that are based on adlineation due to formation of an interface between the platinum and oxide materials, and by spillover due to surface diffusion of intermediates.

Acknowledgements

J. Shim thanks for the financial support of 1999–2000 postdoctoral fellowship from Korea Research Foundation (KRF) Grant.

References

[1] S. Mukerjee, S. Srinivasan, J. Electroanal. Chem. 357 (1993) 201.
[2] J. Hwang, J. Chung, Electrochim. Acta 38 (1993) 2723.
[3] S. Mukerjee, S. Srinivasan, M.P. Soriaga, J. Electrochem. Soc. 142 (1995) 1409.
[4] B.S. Hobbs, A.C.C. Tseung, Nature 222 (1969) 556.
[5] O. Savadogo, P. Beck, J. Electrochem. Soc. 143 (1996) 3842.
[6] O. Savadogo, et al., US Patent 5,298,343 (1994).
[7] A.K. Shukla, M.K. Ravikumar, A.S. Arico, G. Candiano, V. Antonucci, N. Giordano, A. Hamnett, J. Appl. Electrochem. 25 (1995) 528.
[8] B.C. Beard, P.N. Ross, J. Electrochem. Soc. 133 (1986) 1839.
[9] J.P. Radin, J. Electron. Mater. 7 (1978) 47.
[10] K.Y. Chen, A.C.C. Tseung, J. Electrochem. Soc. 143 (1996) 2703.
[11] D.R. Lowde, J.O. Williams, B.D. McNicol, Appl. Surf. Sci. 1 (1978) 215.
[12] E.A. Ticianelli, C.R. Derouin, S. Srinivasan, J. Electroanal. Chem. 251 (1988) 275.
[13] J. Shim, D.-Y. Yoo, J.-S. Lee, Electrochim. Acta 45 (2000) 1943.
[14] C. Rice, Y. Tong, E. Oldfield, W. Wieckowski, Electrochim. Acta 43 (1998) 2825.
[15] P.N. Ross, Surf. Sci. 102 (1981) 463.
[16] P.J. Kulesza, L.R. Faulkner, J. Am. Chem. Soc. 110 (1988) 4905.
[17] P.J. Kulesza, L.R. Faulkner, J. Electroanal. Chem. 259 (1989) 81.
[18] B.S. Hobbs, A.C.C. Tseung, J. Electrochem. Soc. 119 (1972) 580.
[19] B.S. Hobbs, A.C.C. Tseung, J. Electrochem. Soc. 120 (1973) 766.
[20] P.J. Kulesza, L.R. Faulkner, J. Electrochem. Soc. 136 (1989) 707.
[21] A. Parthasarathy, S. Srinivasan, A.J. Appleby, C.R. Martin, J. Electroanal. Chem. 339 (1992) 101.
[22] M. Fleischmann, J. Koryta, H.R. Thirsk, Trans. Faraday Soc. 63 (1969) 1261.
[23] M. Boudart, M.A. Vannice, J.E. Benson, Z. Physik. Chem. N. F. 64 (1969) 171.
[24] J. McHardy, J.O'M. Bockris, J. Electrochem. Soc. 120 (1973) 53.